Proceedings of the ASME 2021
Pressure Vessels & Piping Conference
PVP2021
July 12-16, 2021, Virtual, Online

PVP2021-62249

VIBRATION-ASSISTED FRICTION STIR WELDING OF AA 2024-T3 PLATES

Ibrahim Sabry
Manufacturing Eng. Dept.,
Modern Academy for Engineering and Technology, Cairo, P.O. Box. 11571, Egypt

Abdel-Hamid I. Mourad
Mech. Eng. Dept.
UAE University
Al Ain, P.O. Box. 15551,
United Arab Emirates

Dinu Thomas Thekkuden
Mech. Eng. Dept.
UAE University
Al Ain, P.O. Box. 11571,
United Arab Emirates

Corresponding author: ahmourad@uaeu.ac.ae

ABSTRACT

In this research, the weldability of AA 2024-T3 plates using vibration-assisted friction stir welding (VaFSW) is primarily inspected. The vibration imparted to the fixture holding the specimens in VaFSW differentiates this state-of-art process from the conventional friction stir welding (FSW) technique. For large-scale welding applications, it is ideal to vibrate the tool with the required amplitude and frequency for optimum performance. Due to limitation in applying vibration to the tool in a milling machine, the vibration is imparted to a custom-designed fixture and rig setup. The fixture, which holds the plates rigidly, is mechanically shaken during the friction stir welding process to boost the material strain in the weld region. The VaFSW is performed with 1800 rpm tool rotational speed, 16 mm/min travel speed and at four intermittent levels of vibrational frequencies (10.11 Hz, 13.56 Hz, 16.67 Hz, 25.17 Hz). The welding morphology and mechanical characteristics of joints produced using VaFSW and FSW are presented in the current work. Finally, the results of VaFSW are compared with conventional FSW. Results show that the tensile strength and, hardness in each of the zones – Nugget zone, heat affected zone, and base metal increased with the increase in the vibrational frequency in the vibration-assisted friction stir welding process. In addition, the ductility of the joints increased by the vibration in the vibration-assisted friction stir welding process due to excessive plasticized material resulting in a greater grain dislocation. Moreover, the mechanical characteristics of weld joints enhanced with the increase in the vibrational frequency. However, the tensile strength and hardness of conventional FSWed joint are slightly higher than the joint produced using VaFSW at 10.11 Hz. This study is promising for finding the capability of VaFSW over FSW to produce quality weld joints.

Keywords: Aluminum 2024 alloy; Amplitude; Frequency; Friction stir welding; Vibration; Vibration-assisted friction stir welding.

NOMENCLATURE

BM	Base material
EFSW	Electrical current-aided friction stir welding
FSW	Friction stir welding
HAZ	Heat affected zone
LaFSW	Laser-assisted friction stir welding
NZ	Nugget zone
TMAZ	Thermo-mechanically affected zone
UVeFSW	Ultrasonic vibration-assisted FSW
VaFSW	Vibration assisted friction stir welding
VHD	Vickers hardness

1. INTRODUCTION

Friction welding is a solid-state welding process in which two metals are joined together in the absence of filler material, source of heating and inert environment. The friction stir welding process is never considered a new process since the process has been widely accepted in several industries for producing firm and rigid joints. In the friction welding processes, the mechanical energy is converted into heat energy at the frictional interface initiating the material bonding process. Inertia friction welding, direct drive friction welding, linear friction welding, friction stir welding (FSW) and orbital friction stir welding are commercialized to manufacture tubes and shafts. Each of these variations of the friction welding process meets specific demands in the industries. Moreover, every such process has its advantages and disadvantages. Due to this reason, there has been enormous effort done in past by many researchers to further modify the process and thereby to improve the quality of the friction welded joints [1–4].

However, the friction welding processes have gained popularity only for welding low melting point metals and alloys of aluminium, magnesium, copper, etc. In general, the low melting point of metals limits the fusion arc welding processes with common welding powersources. However, tungsten inert gas welding, and gas metal arc welding processes with the modern powersources can generate stable low heat input arc [5–7]. These powersources (Surface tension transfer, cold metal transfer) are capable of welding aluminium and aluminium alloys. However, the weldability of aluminium alloys is never the same and they exhibit unique characteristics. Also, certain alloys such as aluminium 6000 series are readily weldable, but under certain conditions, they are often susceptible to hot cracking as a result of high heat generated at the arc by the fusion welding processes [8–11]. To prevent the defects, quality assessment of the welded joints is necessary for qualifying the welds [12–15]. The friction stir welding process offers many benefits over the fusion welding process. The former is recommended to weld Aluminium 2xxx and 7xxx series that are difficult to be welded by fusion welding processes. The other benefits include low distortion even in lengthy welds, absence of fuse, porosity, spatter, low shrinkage, highly energy-efficient and outstanding mechanical characteristics as demonstrated by fatigue, tension and bend testing [16,17]. FSW is capable of imparting less deformation and residual stress in the welded components [18–20]. FSW is also proved to impart more fracture toughness compared to arc welding processes. Several criteria for crack growth [21–26] and fracture toughness evaluations [27–33] are suggested forward by researchers in the past. Porosity and brittle attributed defects are less in FSW compared to arc welding processes. However, the presence and size of cracks have a significant role in the fracture toughness of welded joints [34,35]. Besides, the FSWed joints are least prone to stress corrosion cracking compared to arc welding processes due to less stress generated [36,37]. To a certain extent, solid-state welding process especially friction stir welding process has advanced remarkably over the fusion welding processes to be a good choice for those applications dealing with low melting point metals in aerospace, marine, power plant and automotive industries. Several FSW articles dealing with the optimization of parameters and determination of applied loads emphasize the importance of the friction stir process in the joining sector [38,39].

Many attempts were carried out in the past for further advancing the possibilities of effectively utilizing the conventional friction stir welding process with additional techniques. Laser-assisted friction stir welding (LaFSW), electrical current-aided friction stir welding (EFSW), ultrasonic vibration-assisted friction stir welding (UVeFSW) are some of the newly invented techniques proposed for producing quality weld joints. In the case of the laser-assisted friction stir welding process, Campanelli et al. [40] found out that the laser treatment considerably reduces the transverse and longitudinal residual stresses, increases the elongation and microhardness. Sun et al. [41] concluded that preheating using the laser on the advanced side reduces the frictional heat between tool and workpiece whereas preheating on the retreating side results in the maximum heat input. Wada et al. [42] experimentally found out that the laser preheating in the advanced side reduces the torque needed by the tool and the preheating in the retreating side reduces the weld defects significantly. According to Kohn et al. [43], less transverse forces are required by the laser-assisted FSW compared to the conventional friction stir welding process. A similar reduction in the friction stir welding forces was noticed by Liu et al. [44] using an electrically assisted friction stir welding process. Chowdhury et al. [45] proved that the direct current in FSW increased the joint efficiency whereas the alternating current imparted uniform hardness in the advanced and retreating side. In contradiction, Sengupta et al. [46] claimed that the electrically-assisted friction stir welding process can increase the hardness in addition to the joint efficiency. An abrupt change in the boundary between the nugget zone (NZ) and heat affected zone (HAZ) in the conventional FSW process becomes smooth by the addition of electrical effect [47]. These novel techniques are proved to have an effect on the weld quality.

Muhammad and Wu [48] investigated the dissimilar Al/Cu joint produced using an ultrasonic-assisted friction stir welding (UVeFSW) process and found out that the vibration added in FSW reduces the surface roughness and has no effect on the electrical conductivity whereas the strength of dissimilar weld joints depends on the material in the advancing and retreating side. Kumar et al. [49] claimed an increase in the enhancement of surface roughness, interfacial bonding and material mixing by the addition of vibration. Zhao et al. [50] observed an enhanced plastic flow and high strain rate in the leading and trailing side in the ultrasonic-assisted friction stir welding process. Yang et al. [51] stated that the ultrasound in FSW was used to initiate the nucleation process comparatively earlier at low travel speed reducing the incubation period. At the same time, the ratio of nucleation to deformation increases at a higher travel speed. Yu et al. [52] confirm the enhancement of atomic diffusion by the ultrasound while welding using ultrasound vibration-assisted friction stir welding. Further, increased plastic material flow and low working loads without causing any change to the operating temperature are the benefits of ultrasound vibration-assisted friction stir welding process over the traditional FSW [53]. In addition to the lower plunge forces in ultrasonic-assisted FSW, Park [54] found that the plunge force decreases with the increase in the vibrational amplitude. Ruilin et al. [55] stated that the additional vibration affects the temperature field only at higher welding speeds. From the literature studies, the unconventional ultrasonic vibration-assisted friction stir welding techniques described above have demonstrated a major effect on the welded joints.

Literature highlights the wide scope for the developments in the conventional friction stir welding process. Potential capabilities of the vibration-assisted friction welding process are yet to explore on different metal alloys and geometrical configurations. Since the vibration-assisted friction stir welding process is a new non-conventional approach, a comparative analysis of the mechanical and metallurgical characteristics of conventional and vibration-assisted friction stir welding process is demanded for commercializing the technique. The influence of vibrational frequency in the friction stir welding process in terms of strength and hardness is described in the current work. The results of the study are promising for understanding the new technique and weld properties.

2. MATERIALS AND METHODS

AA 2024-T3 plates having 150 mm X 75 mm X 3 mm were used for joining using vibration-assisted friction stir welding (VaFSW) and conventional friction stir welding processes. Table 1 and Table 2 present the chemical composition and mechanical properties of AA 2024-T3 respectively. The longitudinal edges of the samples were thoroughly washed and rinsed with a solution of caustic sodium hydroxide and water to remove oil and debris followed by drying using a cloth. The specimens are fixed to the fixture as shown in figure 1. A system was developed for VaFSW using a 0.75kW AC motor, camshaft and fixture. Schematic representation of vibration-assisted friction stir welding is shown in figure 2. A 0.75 kW AC motor provided the energy for vibrating the fixture and the rotational motion of the engine shaft is converted into a linear fixture motion using a camshaft. The belt was arranged in such a way as to produce vibration with 0.5 mm amplitude to the fixture. The tool is manufactured with a trapezoidal pin and a cylindrical shoulder using tungsten carbide (Figure 3). The hardness of the shoulder following heat treatment was 65 HRC. The geometrical dimensions of the VaFSW and FSW tool are shown in figure 4. Four sets of vibrational frequencies - 10.11 Hz, 13.56 Hz, 16.67 Hz and 25.17 Hz, and fixed rotational and transverse speed of 1800 rpm and 16 mm/min respectively are selected as process parameters (Table 3). Fouladi and Abbasi [56] investigated the friction stir vibration welding process for AA 5052 using frequencies lying between 20 Hz and 40 Hz. However, the vibrational frequency is limited to 25.17 Hz above which resulted in a defective joint. Joints using conventional FSW and VaFSW are prepared. Tensile tests are conducted using cut transverse tensile specimens. Macrostructures with 5X magnification using an optical microscope are observed. Finally, the Vickers hardness (VHD) along different points in the transverse direction is provided.

Table 1 Chemical composition (wt. %) of Al 2024

Element	Al	Si	Fe	Cu	Mn	Mg	Others
Weight (%)	91.1	0.5	0.5	4.4	1.5	1.5	0.5

Table 2 Mechanical properties of AA 2024

Alloy	σ_{UTS} (Mpa)	EL (%)	VHD
2024	400.690	25	120

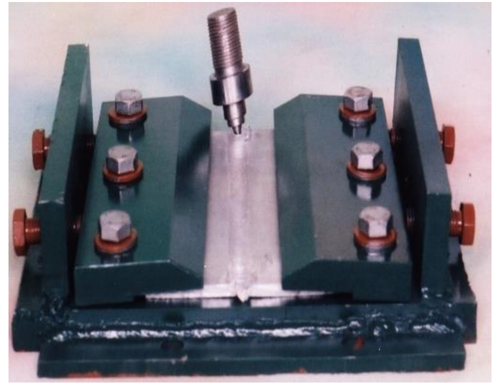

FIGURE 1: FIXTURE USED FOR HOLDING THE SPECIMENS

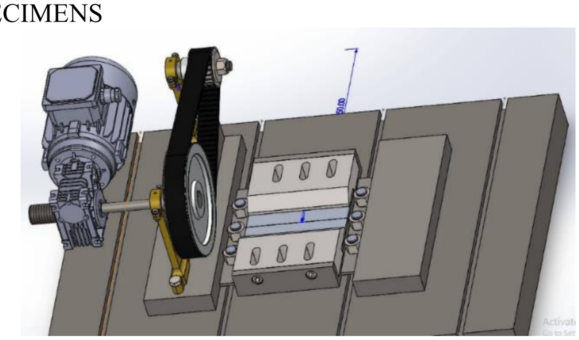

FIGURE 2: SCHEMATIC DESIGN OF VaFSW SETUP

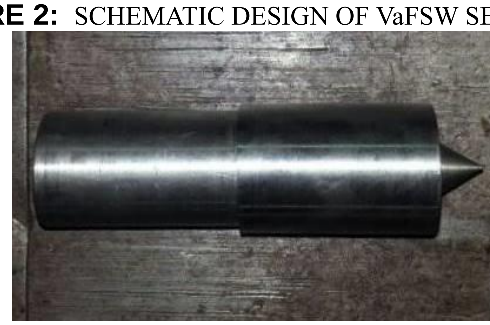

FIGURE 3: TOOL USED FOR FSW AND VaFSW

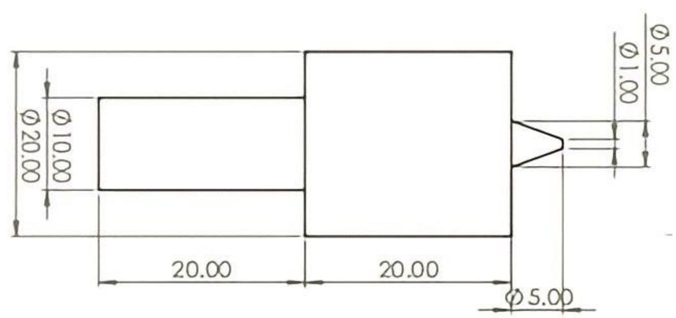

FIGURE 4: GEOMETRICAL DIMENSIONS OF STIRRING TOOL (Units are in mm)

Table 3 VaFSW process parameters

Rotational speed (rpm)	Transverse speed (mm/min)	Vibration (Hz)
1800	16	25.17
1800	16	16.67
1800	16	13.56
1800	16	10.11

3. RESULTS AND DISCUSSION

Smooth and surface defect-free quality joints are produced using FSW and VaFSW. The vibration added to the fixture has not imparted any cracks or defects on the weld surface. According to Shi et al. [57] and Liu et al. [58], the ultrasonic vibrations in the FSW process cause acoustic softening and enhance the plastic material flow to diminish or eliminate the tunnel defects. The absence of tunnel-type defects at the cross-section of weld geometry in the current study supports the findings of Shi et al. [57] and Liu et al. [58]. Lack of defects using the vibration-assisted friction stir welding process indicates the appropriateness of the process for industrial use. However, the estimation of mechanical and metallurgical characteristics of VaFSW compared to FSW is mandatory for the wide acceptance of the technology. Figure 5 shows the macro cross-section of friction stir welded, vibration-assisted friction stir welded joint and base material (BM). The transverse cross-section of the welded specimen was free from any tunnel or pocket defects. Also, pinholes and voids across and along the boundaries of the nugget zone, thermo-mechanically affected zone (TMAZ), heat affected zone and base material are absent in the FSWed and VaFSWed joints [59]. This characteristic indicates the occurrence of proper fusion in FSWed and VaFSWed joints. Besides, the grain size in the nugget zone is appeared as small and dark. The grains in the TMAZ is elongated compared to NZ due to thermal and mechanical effect. Due to the effect of vibration in VaFSW, the TMAZ is slightly broadened making it difficult to distinguish with HAZ and BM. The results are in co-agreement with the work of Liu et al. [60]. The process parameters used for both of the welding processes are optimum since defect-free and quality welds are achieved with the set of parameters used for the current study.

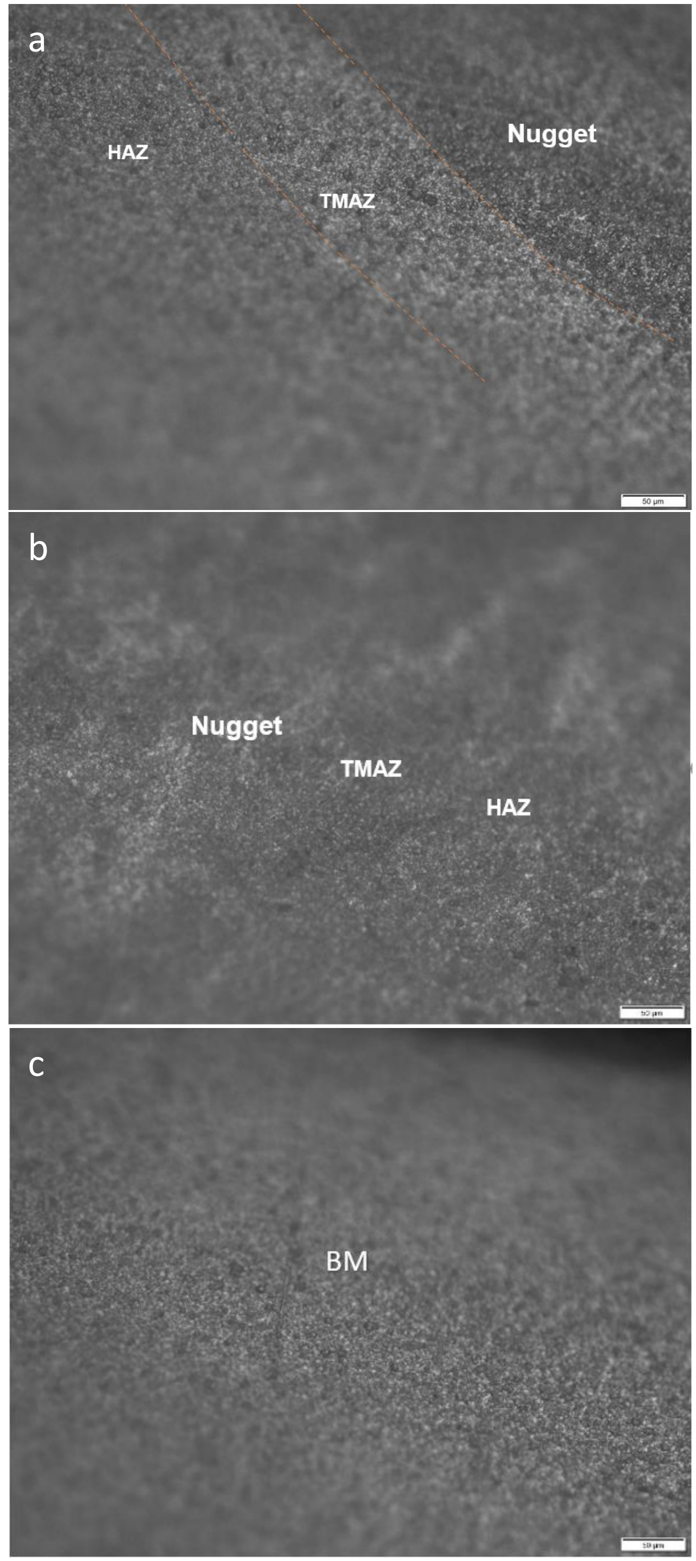

FIGURE 5: MACROSTRUCTURES OF WELDED SPECIMEN (a) FSW (b) VaFSW (c) BASE MATERIAL

The strength, one of the major quality indicative factors, is evaluated by conducting the tensile tests made of transverse tensile test specimens. Figure 6 and figure 7 show the tensile specimens of FSW and VaFSW before and after the fracture. In both cases, the tensile specimens fractured exactly at the welded regions. Hence, the weld strength falls below the base material strength in FSW and VaFSW processes. A comparison showing the stress-strain graphs of all the welded specimens using VaFSW and FSW is shown in figure 8. Table 4 presents the ultimate tensile strength, fracture elongation from the stress-strain graphs and hardness at the nugget zones. These same responses were used by Nirmal and Jagadesh [61] for estimating the quality of dual phase titanium alloys. From the graphs, all the vibration-assisted friction stir welds other than welded at 10.11 Hz have tensile strength and fracture elongation greater than the joint produced by conventional friction stir welding. Since percentage elongation is a measure of ductility, the VaFSW joints produced using vibrational frequencies greater than 13.56 Hz are more ductile compared to the FSW joint. Ding and Wu [62] agree that the strength and ductility of vibration-assisted friction stir welding are slightly higher compared to the conventional friction stir welding process. Similar characteristics with higher tensile strength for the ultrasonic vibration friction stir welded joints compared to FSW joints were attained in the work of Muhammad and Wu [63] that dealt with the joining of aluminium alloy and copper. Moreover, strength and ductility values of VaFSWed specimens at 25.17 Hz vibrational frequency are greater than specimen corresponding to 10.11 Hz. Within the investigated range of vibration frequencies, both the tensile strength and ductility of the VAFSW joints increased with the rise in the vibrational frequencies. These changes in the mechanical characteristics of VaFSW joints are due to grain refinement at the stirring zones and surrounded heat affected regions. This correlation is according to the Hall-Petch relation that says the yield strength increases with the decrease in the grain size [64]. It is proved that the vibration added to the fixture or tool in the case of friction stir welding reduces the grain size in and around the nugget zone due to heat dissipation. This decrease in the grain size resulted in increased strength and ductility of VaFSWed specimens. The results show an increase in the elongation percentage as the vibration frequency increases within the experimented range. This typically indicates an increase in ductility. According to Ma et al. [65] and Estrin et al. [66], the ductility of specimens after friction stir processing increases when the grain size decreases. The volume fraction of grain boundary increases as grain size decreases. These high-volume fraction grain boundaries obstruct the crack growth and enhance the ductility. According to Estrin et al. [66], as grain size decreases, the ductile behaviour in AZ31 magnesium alloy is enhanced by the transition in the fracture mechanism from intergranular fracture to transgranular fracture.

FIGURE 6: FSW TENSILE SPECIMENS BEFORE AND AFTER THE FRACTURE

FIGURE 7: VaFSW TENSILE SPECIMENS BEFORE AND AFTER THE FRACTURE

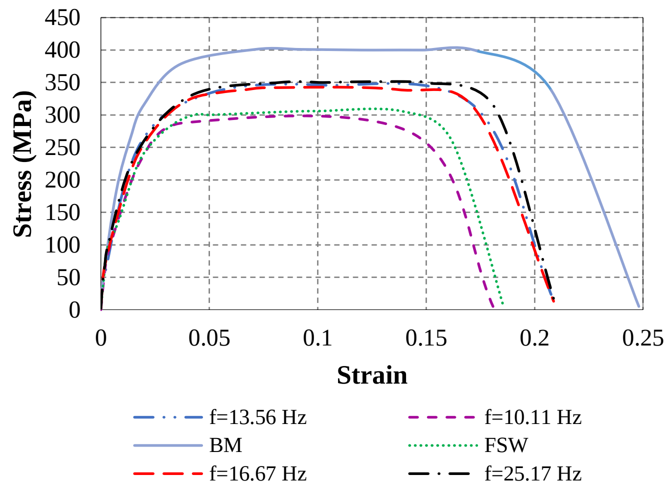

FIGURE 8: STRESS-STRAIN CURVES OF FSWed AND VaFSWed SPECIMENS

Table 4 Mechanical properties of VaFSW specimens

Vibration (Hz)	Ultimate tensile strength (MPa)	Elongation (%)	Hardness (HV)
25.17	350	21.6	96
16.67	344	21.4	94
13.56	334	21.1	93
10.11	296	19.3	88

Figure 9 presents the microhardness profile of AA 2024 welded plates using FSW and VaFSW. The typical ‘W’ shaped profile is observed when the microhardness is measured along the transverse direction of the weld region. The hardness is least in the heat affected zone and highest in the base material away from the nugget zone, whereas the hardness at the nugget zone is slightly higher than at the heat affected zones. Since all the parameters such as rotational speed, transverse speed, tool tilt angle, penetration depth and tool dimensions are constant, it is evident from the results that the vibrational frequencies have a significant effect on the hardness in the nugget and heat affected zone. However, the hardness values are slightly higher when the samples are welded using a conventional friction stir welding process compared to vibration-assisted friction stir welding with 10.11 Hz. Correspondingly, the tensile strength and ductility of samples joined using VaFSW at 10.11 Hz are less compared to the conventional FSW.

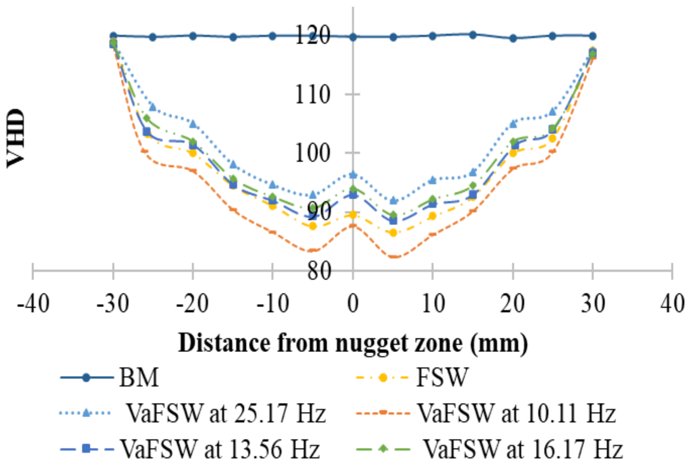

FIGURE 9: MICROHARDNESS VALUES OF VaFSWed AND FSWed SPECIMENS

4. CONCLUSION

A vibration-assisted friction stir welding setup was developed to investigate the influence of vibration on the welded AA 2024 plates. Sound and defect-free joints were produced using both FSW and VaFSW. The results from the comparative study of FSW and VaFSW are listed below.

- The VaFSW and conventional FSW are successful with the experimented process parameters in producing pinholes-free and voids-free weld joints.
- The thermo-mechanically affected zone is broadened in the vibration-assisted friction stir welding compared to conventional FSW.
- The tensile strength and ductility of the VaFSW joints increased with the increase in the vibrational frequencies.
- Vibration-assisted friction stir welds with frequency over 13.56 Hz exhibited higher tensile strength and fracture elongation compared to the sample welded by conventional friction stir welding.
- The tensile strength and hardness of conventional FSWed joint are slightly higher than the joint produced using VaFSW at 10.11 Hz.
- Hardness in the zones of FSWed and VaFSWed specimens is in the order BM>NZ>HAZ
- Vibration frequency is a significant factor affecting the tensile strength, hardness and ductility in a FSW process.

ACKNOWLEDGEMENTS

The authors would like to acknowledge the financial support provided by the United Arab Emirates University through grant number 31R105-Research center.

REFERENCES

[1] I. Sabry, A-H.I. Mourad, D.T. Thekkuden, Optimization of metal inert gas-welded aluminium 6061 pipe parameters using analysis of variance and grey relational analysis, SN Appl. Sci. 2 (2020) 175.

[2] R. Palanivel, P.K. Mathews, N. Murugan, Optimization of process parameters to maximize ultimate tensile strength of friction stir welded dissimilar aluminum alloys using response surface methodology, J. Cent. South Univ. 20 (2013) 2929–2938.

[3] A.M. El-Kassas, I. Sabry, A-H.I. Mourad, D.T. Thekkuden, Characteristics of Potential Sources - Vertical Force, Torque and Current on Penetration Depth for Quality Assessment in Friction Stir Welding of AA 6061 Pipes, Int. Rev. Aerosp. Eng. (IREASE); Vol 12, No 4. (2019). https://www.praiseworthyprize.org/jsm/index.php?journal=irease&amp.

[4] I. Sabry, A-H.I. Mourad, D.T. Thekkuden, Comparison of Mechanical Characteristics of Conventional and Underwater Friction Stir Welding of AA 6063 Pipe Joints, Int. Rev. Mech. Eng. (IREME); Vol 14, No 1. (2020). http://www.praiseworthyprize.org/jsm/index.php?journal=ireme&amp.

[5] P. Kah, R. Suoranta, J. Martikainen, Advanced gas metal arc welding processes, Int. J. Adv. Manuf. Technol. 67 (2013) 655–674.

[6] A-H.I. Mourad, A. Khourshid, T. Sharef, Gas tungsten arc and laser beam welding processes effects on duplex stainless steel 2205 properties, Mater. Sci. Eng. A. 549 (2012) 105–113. https://doi.org/10.1016/j.msea.2012.04.012.

[7] Y. Tang, X. Ye, L. Ding, P. Zhang, Z. Yu, S. Yang, D. Wu, K. Fu, High-temperature tensile properties and interface structure of Ni–Fe dissimilar butt joints welded using the cold metal transfer process, J. Mater. Res. Technol. 9 (2020) 15023–15033.

[8] A.M. Khourshid, I. Sabry, Analysis and design of Friction stir welding, Int. J. Mech. Eng. Rob. Res. (2013) 149–2278.

[9] H.S. Patil, S.N. Soman, Experimental study on the effect of welding speed and tool pin profiles on AA6082-O aluminium friction stir welded butt joints, Int. J. Eng. Sci. Technol. 2 (2010) 268–275.

[10] B. Halverson, J.F. Hinrichs, Friction stir welding (FSW) of littoral combat ship deckhouse structure, J. Sh. Prod. 23 (2007) 161–163.

[11] K.J. Colligan, Friction stir welding for ship construction, Contract. 14 (2004) 1–6.

[12] D.T. Thekkuden, A-H.I. Mourad, J.V. Christy, A.H. Idrisi, Assessment of Weld Quality Using Control Chart and Frequency Domain Analysis, in: ASME 2018 Press. Vessel. Pip. Conf., American Society of Mechanical Engineers, 2018: p. V06BT06A004-V06BT06A004.

[13] D. ThomasThekkuden, A-H.I. Mourad, M.M. Sherif, Response surface analysis of statistical features of voltage and current in a GMAW powersource on welding v-groove joints, in: 2020 Adv. Sci. Eng. Technol. Int. Conf., IEEE, n.d.: pp. 1–6.

[14] D.T. Thekkuden, A-H.I. Mourad, Investigation of feed-forward back propagation ANN using voltage signals for the early prediction of the welding defect, SN Appl. Sci. 1 (2019) 1615.

[15] D.T. Thekkuden, A. Santhakumari, A. Sumesh, A-H.I. Mourad, K. Rameshkumar, Instant detection of porosity in gas metal arc welding by using probability density distribution and control chart, Int. J. Adv. Manuf. Technol. (2018). https://doi.org/10.1007/s00170-017-1484-6.

[16] A.M. Khourshid, I. Sabry, Friction stir welding study on aluminum pipe, Int. J. Mech. Eng. Robot. Res. 2 (2013) 31–339.

[17] D. Sakurada, K. Katoh, H. Tokisue, Underwater friction welding of 6061 aluminum alloy, JOURNAL-JAPAN Inst. Light Met. 52 (2002) 2–6.

[18] V. Dixit, R.S. Mishra, R.J. Lederich, R. Talwar, Influence of process parameters on microstructural evolution and mechanical properties in friction stirred Al-2024 (T3) alloy, Sci. Technol. Weld. Join. 14 (2009) 346–355.

[19] I. Sabry, A.M. El-Kassas, A-H.I. Mourad, D.T. Thekkuden, J. Abu Qudeiri, Friction Stir Welding of T-Joints: Experimental and Statistical Analysis, J. Manuf. Mater. Process. 3 (2019) 38.

[20] C.I. Chang, C.J. Lee, J.C. Huang, Relationship between grain size and Zener–Holloman parameter during friction stir processing in AZ31 Mg alloys, Scr. Mater. 51 (2004) 509–514.

[21] S.K. Maiti, A-H.I. Mourad, Criterion for mixed mode stable crack growth—I. Three point bend geometry, Eng. Fract. Mech. 52 (1995) 321–347.

[22] S.K. Maiti, A-H.I. Mourad, Criterion for mixed mode stable crack growth—II. Compact tension geometry with and without stiffener, Eng. Fract. Mech. 52 (1995) 349–378.

[23] A-H.I. Mourad, S.K. Maiti, Mode II stable crack growth, Fatigue Fract. Eng. Mater. Struct. 19 (1996) 75–84.

[24] A-H.I. Mourad, S.K. Maiti, Influence of state of stress on mixed mode stable crack growth through D16AT aluminium alloy, Int. J. Fract. 72 (1995) 241–258.

[25] A-H.I. Mourad, Pure shear stable crack growth through Compact-Tension-Shear specimen in plane state of stress, Strength, Fract. Complex. 2 (2004) 111–125.

[26] S.K. Maiti, G.K. Kishore, A-H.I. Mourad, Bilinear CTOD/CTOA scheme for characterisation of large range mode I and mixed mode stable crack growth through AISI 4340 steel, Nucl. Eng. Des. 238 (2008) 3175–3185.

[27] A-H.I. Mourad, J. Altarawneha, A.E. Domiaty, Y.J. Chao, F.M. Haggag, Fracture Toughness Measurements From Circumferentially-Notched Pipes Tests, Mater. Perform. Charact. 3 (2014) 305–321.

[28] A-H.I. Mourad, J. Altarawneh, A. El Domiaty, Y.J. Chao, Fracture toughness determined from full-scale pipe, in: ASME 2012 Press. Vessel. Pip. Conf., American Society of Mechanical Engineers Digital Collection, 2012: pp. 125–130.

[29] A-H.I. Mourad, A. Abu-Assi, F.M. Haggag, Y.J. Chao, Novel Technique for Normalizing Load–Displacement Curves in Fracture Testing, Mater. Perform. Charact. 3 (2014) 1–20.

[30] A-H.I. Mourad, A. El-Domiaty, Y.J. Chao, Fracture toughness prediction of low alloy steel as a function of specimen notch root radius and size constraints, Eng. Fract. Mech. 103 (2013) 79–93.

[31] A-H.I. Mourad, K.H. Harib, A. El-Domiaty, Fracture Behavior of Friction Stir Spot Welded Joint, in: ASME 2010 Press. Vessel. Pip. Div. Conf., American Society of Mechanical Engineers, 2010: pp. 205–215.

[32] M. El-Sayed, A. El Domiaty, A-H. I. Mourad, M. Lotfy, Leak Before Break Fracture Assessment for X70 Steel Pressurized Tubes With Axial Surface Crack, in: ASME 2018 Press. Vessel. Pip. Conf., American Society of Mechanical Engineers Digital Collection, 2018.

[33] W.K. Ahmed, A-H.I. Mourad, Fracture assessment of strengthened cracked metallic components using FRP stiffeners, Mech. Compos. Mater. 51 (2015) 301–312.

[34] A-H.I. Mourad, A. El-Domiaty, Notch radius and specimen size effects on fracture toughness of low alloy steel, Procedia Eng. 10 (2011) 1348–1353.

[35] T. Iwashita, K. Azuma, Effects of notch sharpness and depth on brittle fractures in single-edge notched bend specimens, Eng. Fract. Mech. 164 (2016) 60–73. https://doi.org/10.1016/j.engfracmech.2016.07.010.

[36] A.I. Aljoboury, A-H.I. Mourad, A. Alawar, M. Abou Zour, O.A. Abuzeid, Stress corrosion cracking of stainless steels recommended for building brine recirculation pumps, Eng. Fail. Anal. 17 (2010) 1337–1344. https://doi.org/10.1016/j.engfailanal.2010.03.008.

[37] Y.A. Alzafin, A-H.I. Mourad, M.A. Zour, O.A. Abuzeid, Stress corrosion cracking of Ni-resist ductile iron used in manufacturing brine circulating pumps of desalination plants, Eng. Fail. Anal. 16 (2009) 733–739. https://doi.org/10.1016/j.engfailanal.2008.06.013.

[38] S.H. Iftikhar, A-H.I. Mourad, J. Sheikh-Ahmad, An overview of friction stir welding of high-density polyethylene, in: 2020 Adv. Sci. Eng. Technol. Int. Conf., IEEE, n.d.: pp. 1–6.

[39] A-H.I. Mourad, M. Allam, A. El Domiaty, Study on the mechanical behavior of aluminum alloy 5083 friction stir welded joint, in: ASME 2014 Press. Vessel. Pip. Conf., American Society of Mechanical Engineers,

2014: p. V06AT06A014-V06AT06A014.
[40] S.L. Campanelli, G. Casalino, C. Casavola, V. Moramarco, Analysis and comparison of friction stir welding and laser assisted friction stir welding of aluminum alloy, Materials (Basel). 6 (2013) 5923–5941.
[41] Y.F. Sun, Y. Konishi, M. Kamai, H. Fujii, Microstructure and mechanical properties of S45C steel prepared by laser-assisted friction stir welding, Mater. Des. 47 (2013) 842–849.
[42] T. Wada, Y. Morisada, Y. Sun, H. Fujii, Y. Kawahito, M. Matsushita, R. Ikeda, Friction Stir Welding of Medium Carbon Steel with Laser-Preheating, ISIJ Int. 60 (2020) 153–159.
[43] G. Kohn, Y. Greenberg, I. Makover, A. Munitz, Laser-assisted friction stir welding, Weld. J. 81 (2002) 46–48.
[44] X. Liu, S. Lan, J. Ni, Electrically assisted friction stir welding for joining Al 6061 to TRIP 780 steel, J. Mater. Process. Technol. 219 (2015) 112–123.
[45] I. Das Chowdhury, K. Sengupta, D.K. Singh, S. Roy, S. Ghosal, A.K. Mondal, U. Sengupta, Study of mechanical properties of mild steel joint made by electrically assisted friction stir welding using DC and AC, Mater. Today Proc. (2020).
[46] K. Sengupta, D.K. Singh, A.K. Mondal, D. Bose, B. Ghosh, Analysis of mechanical property of electrically assisted friction stir welding to enhance the efficiency of joints, Mater. Today Proc. (2020).
[47] X. Jiang, Y. Han, S. Chen, Y. Bai, T. Yuan, X. Wang, Microstructure and texture investigation on electrically assisted friction stir welded titanium alloy, Mater. Sci. Technol. 36 (2020) 1628–1638.
[48] N.A. Muhammad, C. Wu, Evaluation of capabilities of ultrasonic vibration on the surface, electrical and mechanical behaviours of aluminium to copper dissimilar friction stir welds, Int. J. Mech. Sci. 183 (2020) 105784.
[49] S. Kumar, C. Wu, S. Gao, Process parametric dependency of axial downward force and macro-and microstructural morphologies in ultrasonically assisted friction stir welding of Al/Mg alloys, Metall. Mater. Trans. A. (2020) 1–19.
[50] W. Zhao, C. Wu, H. Su, Numerical investigation of heat generation and plastic deformation in ultrasonic assisted friction stir welding, J. Manuf. Process. 56 (2020) 967–980.
[51] C. Yang, C. Wu, L. Shi, Effect of ultrasonic vibration on dynamic recrystallization in friction stir welding, J. Manuf. Process. 56 (2020) 87–95.
[52] M. Yu, H. Zhao, F. Xu, T. Chen, L. Zhou, X. Song, N. Ma, Influence of ultrasonic vibrations on the microstructure and mechanical properties of Al/Ti friction stir lap welds, J. Mater. Process. Technol. (2020) 116676.
[53] L. Shi, C.S. Wu, L. Fu, Effects of tool shoulder size on the thermal process and material flow behaviors in ultrasonic vibration enhanced friction stir welding, J. Manuf. Process. 53 (2020) 69–83.
[54] K. Park, Development and Analysis of Ultrasonic Assisted Friction Stir Welding Process., (2009).
[55] L. Ruilin, H. Diqiu, L. Luocheng, Y. Shaoyong, Y. Kunyu, A study of the temperature field during ultrasonic-assisted friction-stir welding, Int. J. Adv. Manuf. Technol. 73 (2014) 321–327.
[56] S. Fouladi, M. Abbasi, The effect of friction stir vibration welding process on characteristics of SiO2 incorporated joint, J. Mater. Process. Technol. 243 (2017) 23–30.
[57] L. Shi, C.S. Wu, G.K. Padhy, S. Gao, Numerical simulation of ultrasonic field and its acoustoplastic influence on friction stir welding, Mater. Des. 104 (2016) 102–115.
[58] X. Liu, C. Wu, G.K. Padhy, Characterization of plastic deformation and material flow in ultrasonic vibration enhanced friction stir welding, Scr. Mater. 102 (2015) 95–98.
[59] I. Alinaghian, S. Amini, M. Honarpisheh, Residual stress, tensile strength, and macrostructure investigations on ultrasonic assisted friction stir welding of AA 6061-T6, J. Strain Anal. Eng. Des. 53 (2018) 494–503.
[60] X.C. Liu, C.S. Wu, G.K. Padhy, Improved weld macrosection, microstructure and mechanical properties of 2024Al-T4 butt joints in ultrasonic vibration enhanced friction stir welding, Sci. Technol. Weld. Join. 20 (2015) 345–352.
[61] K. Nirmal, T. Jagadesh, Numerical simulations of friction stir welding of dual phase titanium alloy for aerospace applications, Mater. Today Proc. (2020).
[62] W. Ding, C. Wu, Effect of ultrasonic vibration exerted at the tool on friction stir welding process and joint quality, J. Manuf. Process. 42 (2019) 192–201.
[63] N.A. Muhammad, C.S. Wu, Ultrasonic vibration assisted friction stir welding of aluminium alloy and pure copper, J. Manuf. Process. 39 (2019) 114–127.
[64] P.P.G.E. Dieter, Mechanical Metallurgy. M c Graw-Hill Book Co., New York 1986. XXIII+ 751 p., DM 138.50, ISBN 0–07–016893–8. Crystal Research and Technology, 1988.
[65] Z.Y. Ma, A.L. Pilchak, M.C. Juhas, J.C. Williams, Microstructural refinement and property enhancement of cast light alloys via friction stir processing, Scr. Mater. 58 (2008) 361–366.
[66] Y.Z. Estrin, P.A. Zabrodin, I.S. Braude, T. V Grigorova, N. V Isaev, V. V Pustovalov, V.S. Fomenko, S.E. Shumilin, Low-temperature plastic deformation of AZ31 magnesium alloy with different microstructures, Low Temp. Phys. 36 (2010) 1100–1106.

